

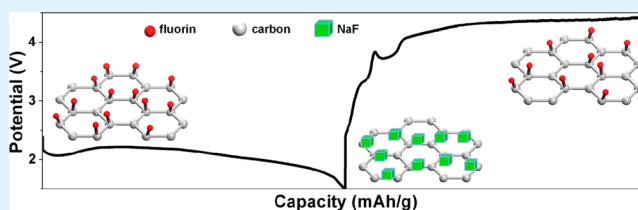
# Rechargeable Room-Temperature CF<sub>x</sub>-Sodium Battery

Wen Liu,<sup>†,§</sup> Hong Li,<sup>‡</sup> Jing-Ying Xie,<sup>\*,§</sup> and Zheng-Wen Fu<sup>\*,†</sup><sup>†</sup>Shanghai Key laboratory of Molecular Catalysts and Innovative materials, Department of Chemistry, Fudan University, Shanghai, P. R. China<sup>‡</sup>Institute of Physics, Chinese Academy of Sciences, Beijing, P. R. China<sup>§</sup>Shanghai Institute of Space Power Sources, Shanghai, P. R. China

## Supporting Information

**ABSTRACT:** Here we demonstrate for the first time that CF<sub>x</sub> cathodes show rechargeable capability in sodium ion batteries with an initial discharge capacity of 1061 mAh g<sup>-1</sup> and a reversible discharge capacity of 786 mAh g<sup>-1</sup>. The highly reversible electrochemical reactivity of CF<sub>x</sub> with Na at room temperature indicates that the decomposition of NaF could be driven by carbon formed during the first discharge. The high reversible capacity made it become a promising cathode material for future rechargeable sodium batteries.

**KEYWORDS:** CF<sub>x</sub>, rechargeable sodium battery, NaF, room temperature, high specific capacity



## 1. INTRODUCTION

Driven by the constant demands on rechargeable batteries with higher energy density and more sustainable economy for energy storage and electric vehicles, great efforts are being directed towards exploring and optimizing light element materials such as sulfur and oxygen with their potential in advantageously offering a high energy density as advanced cathode materials.<sup>1–4</sup> For example, in lithium or sodium–sulfur and lithium or sodium–oxygen/air batteries based on the cathode materials of S and O light elements, the electrons and lithium or sodium are stored at the positive electrode by reacting them with sulfur and oxygen to form lithium or sodium sulfide (Li<sub>2</sub>S or Na<sub>2</sub>S) and Li<sub>2</sub>O<sub>2</sub> or NaO<sub>2</sub>, which ensure a far higher energy density of 300–500 Wh/kg than the lithium-ion counterparts currently used simply (<200 Wh/kg). Theoretically, elemental fluorine (F) as cathode material could also react with lithium or sodium to form LiF or NaF to achieve a high specific capacity of 1411 mAh/g and should hold the same great promise as other cathode materials of S and O. Unfortunately, rechargeable batteries based fluorine seem impossible to be handled and there has been less work about the possibility of rechargeable batteries with fluorine as cathode.

Elemental fluorine is known to react with carbon to yield CF<sub>x</sub>.<sup>5,6</sup> This material was firstly selected as an active cathode in primary lithium batteries,<sup>7</sup> and such primary Li/CF<sub>x</sub> batteries (theoretical energy density was 2189 Wh/kg) with high energy density up to 560 Wh/kg were commercialized by Matsushita Electric Corporation (Japan) in 1975.<sup>8</sup> It has been confirmed that CF<sub>x</sub> will convert into LiF and carbon when reacting with lithium. These primary Li/CF<sub>x</sub> batteries indicated the irreversible reaction of CF<sub>x</sub> with lithium and many attempts for extending the application concepts of CF<sub>x</sub> in lithium ion batteries were made to conclude no any evidence on its

reversibility.<sup>9</sup> The electrochemical reversibility of CF<sub>x</sub> with lithium firstly reported in F-ion battery and a low capacity of less than 120 mAh/g was achieved.<sup>10</sup> Al/CF<sub>x</sub> also purposed for future batteries,<sup>11</sup> other metal fluorides such as FeF<sub>3</sub> or CoF<sub>2</sub> have been intensively studied as electrodes for Li-ion batteries, and exhibited a fascinating conversion reactivity with lithium.<sup>12–19</sup> Here, we demonstrate that CF<sub>x</sub> as cathode material can be applied to rechargeable sodium battery, and the reversible formation and decomposition of NaF could be driven by carbon in Na-CF<sub>x</sub> batteries.

## 2. RESULTS AND DISCUSSION

Details of cathode preparation and cell assembly as well as related physical characterization are provided in the Supporting Information. Figure 1a shows the first discharge–charge curves of Na-CF<sub>x</sub> cell cycled between 1.5 V and 4.4 V at room temperature. The data of Li-CF<sub>x</sub> cell were also included for comparison. CF<sub>x</sub> cathodes in all cells were exposed in argon ambient in order to avoid the effect of air ambient on the electrochemical behaviour of CF<sub>x</sub>. The open-circuit voltages of two cells are close to 2.6 V. During the discharge process of Li-CF<sub>x</sub> cell, a long plateau at about 2.5 V (vs. Li<sup>+</sup>/Li) is observed and agrees well with the previous reports in Li-CF<sub>x</sub>,<sup>20,21</sup> which indicates the formation of LiF. While in Na-CF<sub>x</sub> cell, a discharge voltage plateau appear at 2.4 V (vs. Na<sup>+</sup>/Na), which is lower than the theoretical value of 2.83 V, with NaF as products. This polarization phenomenon was similar to that in the Li-CF<sub>x</sub> cell,<sup>22</sup> which may be caused by the existence of a large activation energy associated with the breaking of the

Received: November 14, 2013

Accepted: February 4, 2014

Published: February 4, 2014

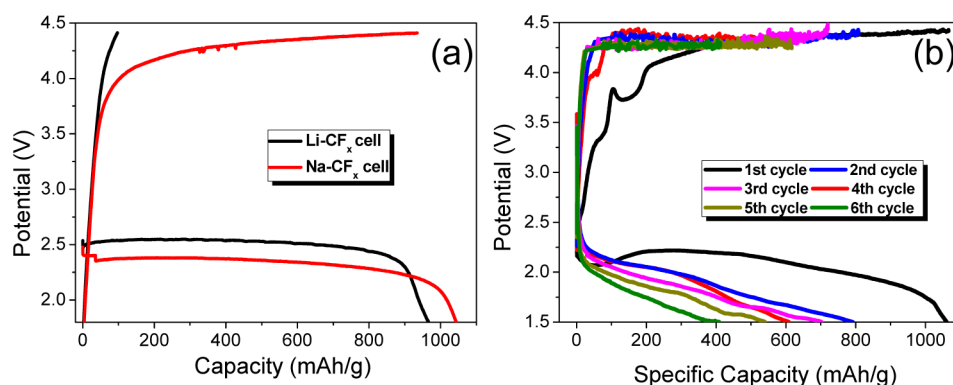


**Figure 1.** (a) Comparison of the first discharge–charge curves of Na-CF<sub>x</sub> cell and Li-CF<sub>x</sub> cell at a current density of 100 mAh/g; (b) Potential profiles and specific discharge/charge capacities of Na-CF<sub>x</sub> cell at a current density of 200 mAh/g.

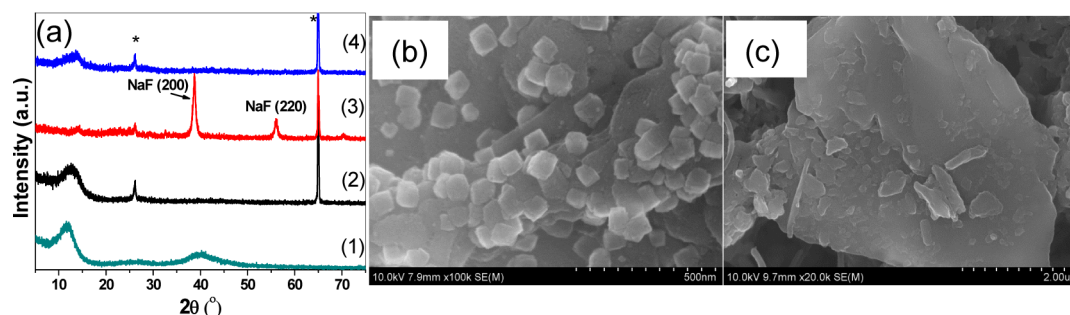


**Figure 2.** (a) XRD patterns of (1) the pure CF<sub>x</sub> powder; (2) a pristine CF<sub>x</sub> electrode; (3) CF<sub>x</sub> electrode after the firstly discharging to 1.5 V; (4) CF<sub>x</sub> electrode after the firstly charging to 4.4 V. SEM image of a CF<sub>x</sub> electrode (b) after the firstly discharging to 1.5 V and (c) after the firstly charging to 4.4 V.

covalent C–F bonds found in CF<sub>x</sub> materials coupled with the anodic oxidation of organic electrolyte solvents by the strongly oxidizing cathode material. On charging, the voltage increases quickly to about 4.4 V in Li-CF<sub>x</sub> cell with a charge capacity of only 95 mAh/g (10% of the initial discharge capacity), reflecting the irreversible of Li-CF<sub>x</sub> cell. As a comparison, the charge voltage of Na-CF<sub>x</sub> cell rises up to 3.6 V in short time, then increases slowly to 4.4 V with a charge capacity of 941 mAh/g (89.6% of the initial discharge capacity), far higher than that of Li-CF<sub>x</sub> cell. In this window from 1.5–4.4 V, the electrolyte containing NaPF<sub>6</sub> is stable (seen in Figure S1 in the Supporting Information), indicating that the charge capacity was attributed to decomposing NaF. Interestingly, Na-CF<sub>x</sub> cell exhibits highly reversible at room temperature. Potential profiles and specific discharge/charge capacities of Na-CF<sub>x</sub> cell at a current density of 200 mAh/g are shown in Figure 1b. The cell was cycled at round-trip efficiency of 100%. A plateau voltage at around 2.25 V with obvious initial voltage delay is observed during the first discharge process, and subsequent discharge processes exhibit a sloping voltage plateaus from 2.3 to 1.5 V. For the initial charge process, the charging voltage profile shows a hump at early stage and then increases to around 4.25 V steadily. The appearance of the hump is related to the sluggish diffusion and reaction kinetics of the charging process for CF<sub>x</sub> electrode. The first discharge capacity of 1061 mAh/g is almost the same as that of Li-CF<sub>x</sub> cell. This discharge process should be attributed to the conversion reaction. In subsequent cycles, the discharge capacities gradually decrease. The discharge capacities are 786 and 409 mAh/g in the second and sixth cycle. These results indicate highly reversible electrochemical reactivity of CF<sub>x</sub> with

Na at room temperature. However, it can be seen that the charge potential is about 4.25 V leading a gap of 2 V between discharge and charge potential. Obviously, Na-CF<sub>x</sub> batteries should be further improved in the future work.

To reveal the electrochemical reaction features of CF<sub>x</sub> with sodium, we performed ex situ SEM, XRD, and XPS measurements on CF<sub>x</sub> electrodes arrested at different stages during the first cycle. Figure 2a shows the ex situ XRD patterns of CF<sub>x</sub> power and CF<sub>x</sub> electrodes: the pristine, that after discharging to 1.5 V and that after charging to 4.4 V, respectively. Two broad peaks corresponding to the fluorinated phase as shown in Figure 2a-1 at around 12 and 40° are in good agreement with previous data,<sup>23,24</sup> indicating an amorphous structure of the pristine CF<sub>x</sub> power. The diffraction peaks of the pristine CF<sub>x</sub> electrode (marked with star) should be attributed to the aluminum substrate (Figure 2a-2). When the electrode was firstly discharged to 1.5 V, the original broad peak of CF<sub>x</sub> disappeared (Figure 2a-3), and two new diffraction peaks at 38.7 and 56.0° could be well assigned to the (200) and (220) reflection of NaF (JCPDS card no. 04-0793). This finding indicates the decomposition of CF<sub>x</sub> and the formation of NaF after discharge progress. Interestingly, diffraction peaks from NaF disappeared while one broad peak at around 12° appeared again after charging to 4.4 V (Figure 2a-4), indicating the decomposition of NaF and reconstruction of an amorphous structure after charging to 4.4 V. Figure 2b shows the SEM image of CF<sub>x</sub> electrode after the first discharging to 1.5 V, with significant amount of cubic shaped particles protruding from the surface. The size of the particles was about 70 nm. The surface of the pristine CF<sub>x</sub> electrode (seen in Figure S2 in the Supporting Information) is smooth macroscopically for the

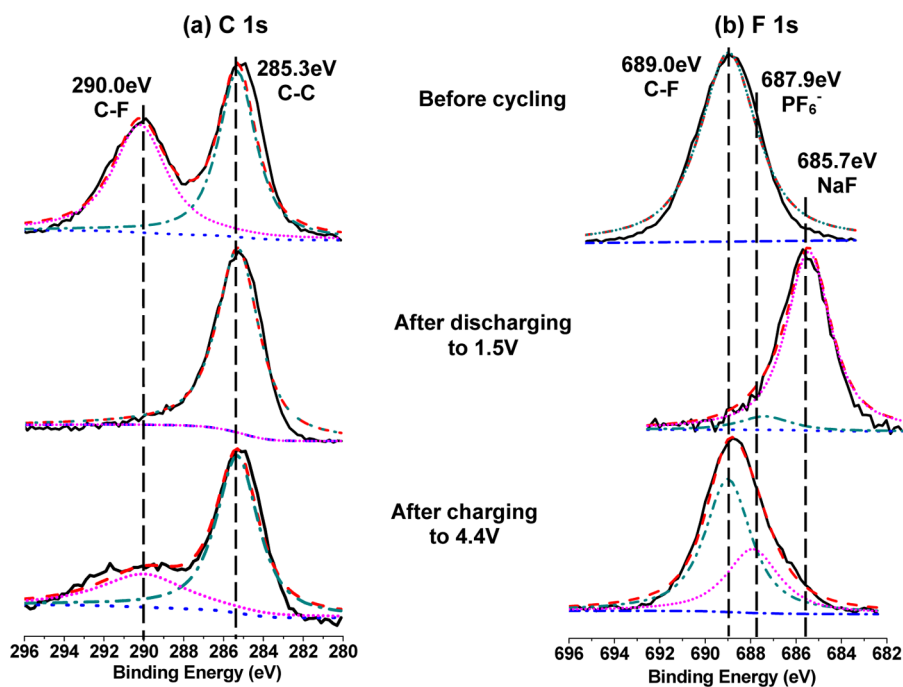


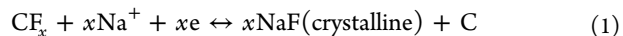
**Figure 3.** XPS spectra of (a) C 1s and (b) F 1s of  $\text{CF}_x$  electrodes at different stages of the first cycle: before cycling; after discharging to 1.5 V; after charging to 4.4 V.

comparison. Thus, it can be concluded that these cubic shaped particles formed during the discharge process were the discharge products, which consist of NaF (see Figure S3 in the Supporting Information). After charging to 4.4 V, the surface of  $\text{CF}_x$  electrode became much smoother than that after discharge even though there are some spots which are not cubic-shaped crystals obviously as shown in Figure 2c. The cubic products disappear totally. This result provides clear evidence that the discharge products of NaF can be decomposed during charge process (see Figure S4 in the Supporting Information). This result is well-consistent with the XRD data, which can be further confirmed by ex situ XPS data.

XPS spectra of C 1s and F 1s for the  $\text{CF}_x$  electrode at different discharge/charge stages of the first cycle are presented in panels a and b in Figure 3, respectively. For the pristine sample, the peaks at 285.3 and 290.0 eV in C 1s spectrum (Figure 3a) correspond to C–C and C–F in  $\text{CF}_x$ , the peak at 689.0 eV in F 1s spectrum can be assigned to C–F. When Na- $\text{CF}_x$  cell was fully discharged to 1.5 V, the C 1s and F 1s spectra were changed obviously. The peak at 290.0 eV in C1s spectrum and the peak at 689.0 eV in F 1s spectrum disappear simultaneously, which reveals reaction of C–F bond with sodium. Furthermore, a new strong signal at 685.7 eV and a weak signal at 687.9 eV in F 1s spectrum appear. They can be attributed to NaF and  $\text{PF}_6^-$  conducting salt in the electrolyte, respectively. This result is well consistent with the analyses from XRD (Figure 2) and EDX (see Figure S3 in the Supporting Information). After charging to 4.4 V, C 1s spectrum and F 1s spectrum are utterly different from those of electrode after discharging to 1.5 V. The peak of C 1s spectrum at 290.0 eV and the peak of F 1s spectrum at 689.0 eV appear again, which should be attributed to the generation of C–F bond renewedly. At the same time, the disappearance of the peak at 685.7 eV in F 1s spectrum indicates that NaF is decomposed. This is consistent with the results from SEM, XRD and EDX (see Figure S4 in the Supporting Information). But after fully

charged, the peak intensity of C–F at 290.0 eV is still weaker than that of the pristine  $\text{CF}_x$  sample, which may be attributed to the dissolution of part of fluorine in the electrolyte, thus results in the loss of active material and the fading of the discharge capacity.

The reversible electrochemical reaction mechanism of sodium with  $\text{CF}_x$  involving the reversible formation and decomposition of NaF is proposed



Electrochemical conversion reaction of  $\text{CF}_x$  with Na may be similar to that of transition metal fluoride with Li. The stable NaF was electrochemically active and can be reversibly decomposed in the interaction with carbon at the voltage range from 1.5–4.4 V. However, the electromotive force to decompose NaF can be found to be 5.65 eV according to Nerst equation and related thermodynamic data (see Table S1 in the Supporting Information). Thus, the carbon framework should act as a mini-reaction chamber, encouraging a conversion reaction of NaF into  $\text{CF}_x$ . This reversible reaction is thermodynamically feasible as the reaction of lithium with  $\text{CF}_x$  (see Table S1 in the Supporting Information). However, the conventional view about the irreversible reaction of  $\text{CF}_x$  with lithium was further confirmed by our own failed attempts (Figure 1a) to electrochemically decompose LiF. The difference between driving the decomposition of NaF and LiF electrochemically by carbon is amazing. This should be due to the fact that the crystallize size of NaF (about 70 nm) is less than that of LiF (around 150 nm, see Figure S5 in the Supporting Information) formed after discharge process, resulting in the better kinetically electrochemical process to decompose NaF than LiF considering higher ion conductivity of NaF (see Table S1 in the Supporting Information). On the other hand, the bond energy and dissociation energy of NaF are lower than that of LiF (see Table S1 in the Supporting Information), the decomposition of NaF need lower energy

than that of LiF from the thermodynamical view. Apparently, the electrochemical driven size confinement of electroactive species should be considered to improve the conversion reversibility of Na-CF<sub>x</sub> cell.

On the basis of eq. 1, our finding indicates that CF<sub>x</sub> is one of the so-called “conversion reaction” materials in sodium ion batteries. So CF<sub>x</sub> also suffers from the high voltage-polarization between charge and discharge, and poor cycle performance as well as poor discharge curves existing in “conversion reaction” materials.<sup>12–15,25</sup> However, the high specific capacity and much higher discharge potential make CF<sub>x</sub> material become a promising cathode material for future rechargeable sodium batteries (see Table S2 in the Supporting Information). Further development is needed on this system to resolve these problems for practical uses.

### 3. CONCLUSIONS

In conclusion, the decomposition of discharge products NaF in the charge process indicates the reversibility of Na-CF<sub>x</sub> cell. The highly reversible electrochemical reactivity of CF<sub>x</sub> with Na at room temperature led to the interesting conclusion that the reversible formation and decomposition of NaF could be driven by carbon formed during the first discharge progress. A highly reversible electrochemical reactivity of CF<sub>x</sub> with Na makes Na-CF<sub>x</sub> cells become a new generation of batteries that have a higher energy density and more sustainable economy.

### ■ ASSOCIATED CONTENT

#### Supporting Information

Assembly and electrochemical measurements of CF<sub>x</sub>/Na cell; CV curve of electrolyte; SEM and EDX of CF<sub>x</sub> electrode; SEM image of CF<sub>x</sub> electrode in Li batteries. This information is available free of charge via the Internet at <http://pubs.acs.org/>.

### ■ AUTHOR INFORMATION

#### Corresponding Authors

\*E-mail: xiejingying2007@126.com, Fax: 21-24188008. Tel: (+86)-21-24187673.

\*E-mail: zwf@fudan.edu.cn. Fax: 21-65642522. Tel: (+86)-21-65642522.

#### Notes

The authors declare no competing financial interest.

### ■ ACKNOWLEDGMENTS

This work was financially supported by the 973 Program (2011CB933300) of China; Science & Technology Commission of Shanghai Municipality (08DZ2270500 and 11JC1400500); Talents of Shanghai (12XD1421900); 863 Program (2013AA050902) of China; and Natural Science Foundation of China (21373137).

### ■ REFERENCES

- (1) Zu, C. X.; Li, H. *Energy Environ. Sci.* **2011**, *4*, 2614–2624.
- (2) Bruce, P. G.; Freunberger, S. A.; Hardwick, L. J. *Nat. Mater.* **2012**, *11*, 19–29.
- (3) Hartmann, P.; Bender, C. L.; Vracar, M. *Nat. Mater.* **2013**, *12*, 228–232.
- (4) Wang, J.; Yang, J.; Nuli, Y. *Electrochem. Commun.* **2007**, *9*, 31–34.
- (5) Ruff, O.; Bretschneider, O.; Anorg, Z. *Allg. Chem.* **1934**, *217*, 1–18.
- (6) Nakajima, T. *J. Fluorine Chem.* **1999**, *100*, 57–61.
- (7) N. Watanabe, M. Fukuda, U.S. Patent 3 536 532, 1970 and 3 700 502, 1972.

(8) Fukuda, M.; Iijima, T. In Collins, D.H., Ed.; *Power Sources 5*; Academic Press: New York, 1975; p 713.

(9) Amatucci, G. G.; Pereira, N. *J. Fluorine Chem.* **2007**, *128*, 243–262.

(10) R. Yazami, *US 2009/0029237 A1*, 2009.

(11) Armand, M.; Tarascon, J. M. *Nature* **2008**, *451*, 652–657.

(12) Liu, P.; Vajo, J. J.; Wang, J. S. *J. Phys. Chem. C* **2012**, *116*, 6467–6473.

(13) Li, T.; Li, L.; Cao, Y. L. *J. Phys. Chem. C* **2010**, *114*, 3190–3195.

(14) Badway, F.; Cosandey, F.; Pereira, N.; Amatucci, G. G. *J. Electrochem. Soc.* **2003**, *150*, A1318–A1327.

(15) Hayner, C. M.; Zhao, X.; Kung, H. H. *Annu. Rev. Chem. Biomol. Eng.* **2012**, *3*, 445–471.

(16) Li, C. L.; Yin, C.; Mu, X.; Maier, J. *Chem. Mater.* **2013**, *25*, 962–969.

(17) Li, C. L.; Yin, C.; Gu, L.; Dinnebier, R. E.; Mu, X.; van Aken, P. A.; Maier, J. *J. Am. Chem. Soc.* **2013**, *135*, 11425–11428.

(18) Nishijima, M.; Gocheva, I. D.; Okada, S.; Doi, T.; Yamaki, J.; Nishida, T. *J. Power Sources* **2009**, *190*, 558–562.

(19) Cabana, J.; Monconduit, L.; Larcher, D.; Palacin, M. R. *Adv. Mater.* **2010**, *22*, E170–E192.

(20) Read, J.; Collins, E.; Piekarski, B. *J. Electrochem. Soc.* **2011**, *158*, A504–A510.

(21) Zhang, S. S.; Foster, D.; Wolfenstine, J. J. *Power Sources* **2009**, *187*, 233–237.

(22) Tiedemann, W. *J. Electrochem. Soc.* **1974**, *121*, 1308–1311.

(23) Lam, P.; Yazami, R. *J. Power Sources* **2006**, *153*, 354–359.

(24) Xiao, J.; Xu, W.; Wang, D.; Zhang, J. G. *J. Electrochem. Soc.* **2010**, *157*, A294–A297.

(25) Aizpurua, F. M.; Laruelle, S.; Grugeon, S.; Tarascon, J. M.; Palacin, M. R. *J. Appl. Electrochem.* **2010**, *40*, 1365–1370.